

# Novel Oxorhenium and Oxotechnetium Complexes from an Aminothiols[NS]/Thiols[S] Mixed-Ligand System

Penelope Bouziotis,<sup>[a]</sup> Ioannis Pirmettis,<sup>[a]</sup> Maria Pelecanou,<sup>[b]</sup> Catherine P. Raptopoulou,<sup>[c]</sup> Aris Terzis,<sup>[c]</sup> Minas Papadopoulos,<sup>[a]</sup> and Efstratios Chiotellis\*<sup>[a]</sup>

**Abstract:** The simultaneous action of a bidentate aminothiols ligand, L<sup>n</sup>H, ( $n = 1$ : (CH<sub>3</sub>CH<sub>2</sub>)<sub>2</sub>NCH<sub>2</sub>CH<sub>2</sub>SH and  $n = 2$ : C<sub>5</sub>H<sub>10</sub>NCH<sub>2</sub>CH<sub>2</sub>SH) and a monodentate thiol ligand, LH (LH: *p*-methoxythiophenol) on a suitable MO (M = Re, <sup>99g</sup>Tc) precursor results in the formation of complexes of the general formula [MO(L<sup>n</sup>)(L)<sub>3</sub>] (**1**, **2** for Re and **5**, **6** for <sup>99g</sup>Tc). In solution these complexes gradually transform to [MO(L<sup>n</sup>)(L)<sub>2</sub>] complexes (**3**, **4** for Re and **7**, **8** for <sup>99g</sup>Tc). The transformation is much faster for oxotechnetium than for oxorhenium complexes. Complexes **1–4**, **7**, and **8** have been isolated and fully characterized by elemental analysis and spectroscopic methods. Detailed NMR assignments were made for complexes **3**, **4**, **7**, and **8**. X-ray studies have demonstrated that the coordination geometry around rhenium in complex **1** is square pyramidal ( $\tau = 0.06$ ), with four sulfur atoms (one from the L<sup>n</sup>H ligand and three from three molecules of *p*-methoxythiophenol) in the basal plane and the oxo group in the apical position. The L<sup>n</sup>H ligand acts as a monodentate ligand with the nitrogen atom being protonated and hydrogen bonded to the oxo group. The four thiols are deprotonated during complexation resulting in a complex with an overall charge of zero. The coordination geometry around rhenium in complex **4** is trigonally distorted square pyramidal ( $\tau = 0.41$ ), while in the oxotechnetium complex **7** it is square pyramidal ( $\tau = 0.16$ ). In both complexes L<sup>n</sup>H acts as a bidentate

ligand. The NS donor atom set of the bidentate ligand and the two sulfur atoms of the two monodentate thiols define the basal plane, while the oxygen atom occupies the apical position. At the technetium tracer level (<sup>99m</sup>Tc), both types of complexes, [<sup>99m</sup>TcO(L<sup>n</sup>)(L)<sub>3</sub>] and [<sup>99m</sup>TcO(L<sup>n</sup>)(L)<sub>2</sub>], are formed as indicated by HPLC. At high ligand concentrations the major complex is [<sup>99m</sup>TcO(L<sup>n</sup>)(L)<sub>3</sub>], while at low concentrations the predominant complex is [<sup>99m</sup>TcO(L<sup>n</sup>)(L)<sub>2</sub>]. The complexes [<sup>99m</sup>TcO(L<sup>n</sup>)(L)<sub>3</sub>] transform to the stable complexes [<sup>99m</sup>TcO(L<sup>n</sup>)(L)<sub>2</sub>]. This transformation is much faster in the absence of ligands. The complexes [<sup>99m</sup>TcO(L<sup>n</sup>)(L)<sub>2</sub>] are stable, neutral, and also the predominant product of the reaction when low concentrations of ligands are used, a fact that is very important from the radiopharmaceutical point of view.

**Keywords:** mixed-ligand approach • NMR spectroscopy • rhenium • structure elucidation • technetium

## Introduction

Technetium, an element belonging to Group 7 of the Periodic Table, has been extensively used in formulating diagnostic

radiopharmaceuticals for scintigraphy and single-photon computed tomography (SPECT) imaging studies in patients.<sup>[1]</sup> In the last 15 years more has been learned about Tc chemistry than in all the previous years since its discovery in 1937. This has resulted in the preparation of a great number of novel <sup>99m</sup>Tc compounds and has produced many useful radiopharmaceuticals with a tremendous impact on the development of diagnostic nuclear medicine. Technetium radiopharmaceuticals like <sup>99m</sup>Tc-HMPAO, <sup>99m</sup>Tc-ECD, <sup>99m</sup>Tc-MIBI, <sup>99m</sup>Tc-MAG<sub>3</sub>, and <sup>99m</sup>Tc-tetrofosmin are now common diagnostic tools.

Rhenium, which also belongs to Group 7, exhibits many of the chemical properties of technetium<sup>[2]</sup> and investigations of rhenium coordination chemistry are often performed in conjunction with technetium, providing a non-radioactive alternative to working with technetium radioisotopes. Furthermore, the  $\beta$ -emitting radionuclides <sup>186</sup>Re and <sup>188</sup>Re are of great interest to nuclear medicine as they possess physical and nuclear properties favorable for use in systemic radiother-

[a] Dr. E. Chiotellis, Dr. P. Bouziotis, Dr. I. Pirmettis, Dr. M. Papadopoulos  
Institute of Radioisotopes—Radiodiagnostic Products  
National Center for Scientific Research “Demokritos”  
15310 Ag. Paraskevi, Athens (Greece)  
Fax: (+301) 6524-480  
E-mail: echiot@mail.demokritos.gr

[b] Dr. M. Pelecanou  
Institute of Biology  
National Center for Scientific Research “Demokritos”  
15310 Ag. Paraskevi, Athens (Greece)

[c] Dr. C. P. Raptopoulou, Dr. A. Terzis  
Institute of Materials Science  
National Center for Scientific Research “Demokritos”  
15310 Ag. Paraskevi, Athens (Greece)

Supporting information for this article is available on the WWW under <http://www.wiley-vch.de/home/chemistry/> or from the author.

apy.<sup>[3]</sup> Further studies on the chemistry of technetium and rhenium will eventually lead to the design of suitable backbones that will be used for the optimum labeling of specific peptides and biomolecules. Therefore, these studies play an important role in the development of novel diagnostic and therapeutic radiopharmaceuticals.

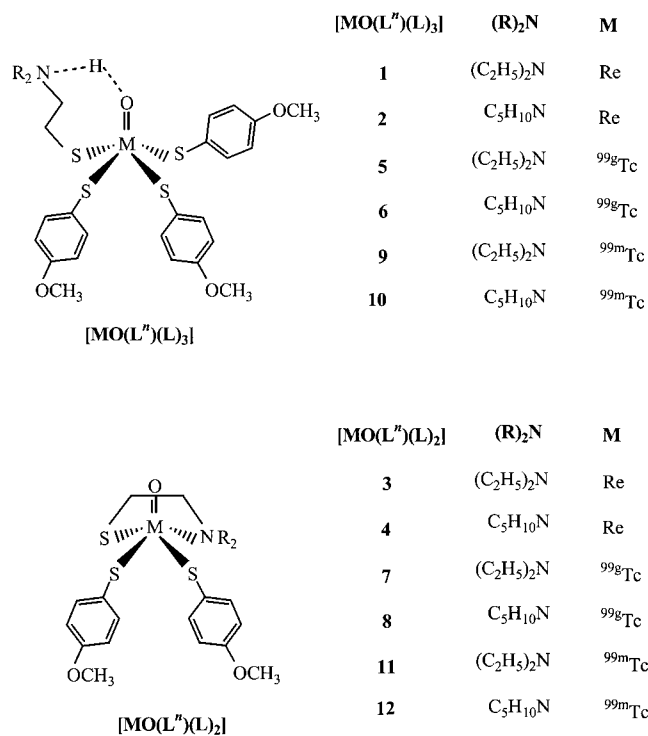
Many studies have recently been reported on the design of mixed-ligand oxorhenium and/or oxotechnetium complexes containing monothiolato and tridentate derivatized thiolato ligands in a “3+1” combination.<sup>[4]</sup> The major advantage of the mixed-ligand system is the ease with which one ligand can be substituted for another, resulting in a wide variety of “3+1” mixed-ligand complexes. These compounds have been biologically evaluated as brain perfusion agents<sup>[5]</sup> or as specific radiopharmaceuticals for brain receptor imaging.<sup>[6]</sup> Since sulfhydryl-containing ligands provide ideal molecules for the synthesis of oxorhenium and oxotechnetium complexes, our interest is currently focused<sup>[7]</sup> on the investigation of other mixed-ligand systems that contain thiol residues, among which are the bidentate aminothiols [NS] and monodentate thiol [S] ligand systems. In contrast to the “3+1” mixed-ligand system SN(R)S/S,<sup>[5, 8]</sup> the formation of stereoisomers can be avoided by symmetric substitution on the nitrogen of the aminothiols ligand, while the advantages of the “3+1” system still remain.

In the present study we report the synthesis and characterization of novel oxorhenium and oxotechnetium complexes of the general formulae  $[\text{MO}(\text{L}^n)(\text{L})_3]$  and  $[\text{MO}(\text{L}^n)(\text{L})_2]$ , in

### Abstract in Greek:

Η ταυτόχρονη επίδραση μιας διδραστικής θειόλης,  $\text{L}^n\text{H}$ , ( $n=1$ :  $(\text{CH}_3\text{CH}_2)_2\text{NCH}_2\text{CH}_2\text{SH}$  και  $n=2$ :  $\text{C}_5\text{H}_{10}\text{NCH}_2\text{CH}_2\text{SH}$ ) και μιας μονοδραστικής θειόλης, LH (LH: *p*-methoxythiophenol) σε μία κατάλληλη πρόδρομη ένωση του ReO δίνει σύμπλοκα του γενικού τύπου  $\text{ReOL}^n/(\text{L})_3$  ή  $\text{ReOL}^n/(\text{L})_2$  (1 ή 2). Τα σύμπλοκα είναι σταθερά στην στερεή φάση αλλά σε διάλυμα μετατρέπονται σταδιακά σε σύμπλοκα του γενικού τύπου  $\text{ReOL}^n/(\text{L})_2$  ή  $\text{ReOL}^n/(\text{L})_2$  όπως επιβεβαιώθηκε με HPLC και NMR. Τα δύο σύμπλοκα σχηματίζονται σε επίπεδο τεχνητίου-99g. Τα δύο σύμπλοκα σχηματίζονται σε επίπεδο τεχνητίου-99g χρησιμοποιώντας σαν πρόδρομο σύμπλοκο το  $^{99g}\text{TcO-glucuronate}$  ( $^{99g}\text{TcOL}^n/(\text{L})_3$ , 5, ή  $^{99g}\text{TcOL}^n/(\text{L})_2$ , 6, και  $^{99g}\text{TcOL}^n/(\text{L})_2$ , 7, ή  $^{99g}\text{TcOL}^n/(\text{L})_2$ , 8) όπως αποδεικνύεται με την HPLC. Όμως, με την πάροδο του χρόνου τα σύμπλοκα 5 και 6 μετατρέπονται εξ' ολοκλήρου στα σύμπλοκα 7 και 8 αντίστοιχα. Τα σύμπλοκα 1, 2, 4, 7, και 8 απομονώθηκαν και χαρακτηρίστηκαν πλήρως με στοιχειακή ανάλυση και φασματοσκοπικές μεθόδους. Κρυσταλλογραφία ακτίνων-Χ έδειξε ότι η γεωμετρία του συμπλόκου 1 είναι τετραγωνική πυραμίδα ( $\tau = 0.06$ ), με τέσσερα άτομα θείου να σχηματίζουν την βάση της πυραμίδας και η οξο ομάδα να καταλαμβάνει την κορυφή της πυραμίδας. Το  $\text{L}^n\text{H}$  δρα σαν μονοδραστικός υποκαταστάτης, το άζωτο είναι πρωτονιωμένο και υπάρχει δεσμός υδρογόνου με την οξο ομάδα. Έτσι, με την αποπρωτονίωση των τεσσάρων θειολών κατά την αντίδραση συναρμογής, το μόριο είναι ουδέτερο. Η γεωμετρία του 4 είναι τριγωνική παραμορφωμένη τετραγωνική πυραμίδα ( $\tau = 0.41$ ) ενώ η γεωμετρία του 7 είναι τετραγωνική πυραμίδα ( $\tau = 0.16$ ). Στα δύο σύμπλοκα το βασικό επίπεδο της πυραμίδας ορίζεται από το άτομο του S και του N του διδραστικού υποκαταστάτη,  $\text{L}^n\text{H}$ , και δύο άτομα S από δύο μονοδραστικές θειόλες. Η οξο ομάδα καταλαμβάνει την κορυφή της πυραμίδας και στα δύο σύμπλοκα. Οι τρεις θειόλες αποπρωτονιώνονται κατά την διάρκεια της συναρμογής και τα σύμπλοκα είναι ουδέτερα. Ιδίας δομής σύμπλοκα ( $^{99m}\text{TcOL}^n/(\text{L})_3$  και  $^{99m}\text{TcOL}^n/(\text{L})_2$ ) σχηματίζονται σε επίπεδο ιχνηθέτη ( $^{99m}\text{Tc}$ ) και η μεταξύ τους αναλογία εξαρτάται από την συγκέντρωση των χημικών υποκαταστάτων. Σε χαμηλές συγκεντρώσεις, το κύριο προϊόν της αντίδρασης είναι το  $^{99m}\text{TcOL}^n/(\text{L})_2$  σύμπλοκο, το οποίο είναι σταθερό σε υδατικό περιβάλλον. Το γεγονός αυτό δείχνει ότι το σύστημα  $^{99m}\text{TcOL}^n/(\text{L})_2$  μπορεί να χρησιμοποιηθεί για την ανάπτυξη ραδιοφάρμακων.

which  $\text{M} = \text{Re}$ ,  $^{99g}\text{Tc}$ , and  $^{99m}\text{Tc}$ . A bidentate aminothiols ligand,  $\text{L}^n\text{H}$  ( $n=1$ :  $(\text{CH}_3\text{CH}_2)_2\text{NCH}_2\text{CH}_2\text{SH}$  and  $n=2$ :  $\text{C}_5\text{H}_{10}\text{NCH}_2\text{CH}_2\text{SH}$ ), and a monodentate thiol ligand, LH (LH: *p*-methoxythiophenol), react with a suitable  $\text{Re}^{\text{VO}}$  or  $^{99g}\text{Tc}^{\text{VO}}$  precursor to produce neutral oxorhenium and oxotechnetium complexes. The aminothiols  $\text{L}^n\text{H}$  acts as a monodentate ligand coordinating only through the sulfur atom, while three aromatic monothiols, LH, occupy the three vacant positions of the equatorial plane, producing  $[\text{MO}(\text{L}^n)(\text{L})_3]$  complexes of the [S][S]<sub>3</sub> type (Scheme 1,



Scheme 1. Structures of the mixed ligand complexes.

complexes 1, 2, 5, and 6). In solution, the nitrogen of the  $\text{L}^n\text{H}$  ligand subsequently coordinates to the metal core with the expulsion of one monodentate thiol to give  $[\text{MO}(\text{L}^n)(\text{L})_2]$  complexes of the [NS][S]<sub>2</sub> type, “2+1+1” combination (Scheme 1, complexes 3, 4, 7, and 8). Both types of complexes have been isolated and fully characterized for rhenium. Although both types of complexes are formed for the technetium carrier ( $^{99g}\text{Tc}$ ), only the complexes  $[\text{ReO}(\text{L}^n)(\text{L})_2]$  have been isolated. For the technetium tracer ( $^{99m}\text{Tc}$ ) both types of complexes are also formed, as indicated by HPLC studies, with the ratio between  $[\text{ReO}(\text{L}^n)(\text{L})_3]$  and  $[\text{ReO}(\text{L}^n)(\text{L})_2]$  greatly dependent on the concentration of ligands in the reaction mixture.

## Results

The synthesis of the bidentate ligands was performed according to reported procedures.<sup>[9]</sup>

**Synthesis and isolation of  $[\text{ReO}(\text{L}^n)(\text{L})_3]$  and  $[\text{ReO}(\text{L}^n)(\text{L})_2]$  complexes:** Three methods were successfully employed for the synthesis of the oxorhenium mixed-ligand complexes. The

synthesis of the complexes was based on ligand exchange reactions with  $[\text{ReOCl}_3(\text{PPh}_3)_2]$ ,<sup>[10]</sup> rhenium(v) gluconate,<sup>[11]</sup> or rhenium(v) citrate<sup>[12]</sup> as precursors (Experimental Section, Methods A–C) in the presence of an equimolar quantity of the bidentate ligand  $\text{L}^n\text{H}$  and an excess of monodentate thiol LH (molar ratio of Re-precursor/ $\text{L}^n\text{H}$ /LH = 1:1:3). Rhenium(v) citrate and rhenium(v) gluconate were used in situ as formed by reduction of  $\text{ReO}_4^-$  by  $\text{Sn}^{\text{II}}$ . The in situ method is commonly used in the development of rhenium radiopharmaceuticals because radioactive rhenium comes in the form of perrhenate salt. All three methods gave approximately the same yield of product.

The reaction products were extracted in dichloromethane. In each case, HPLC analysis of the crude reaction mixture revealed the presence of one product peak with a retention time of approximately 18 minutes (Figure 1 trace A). After

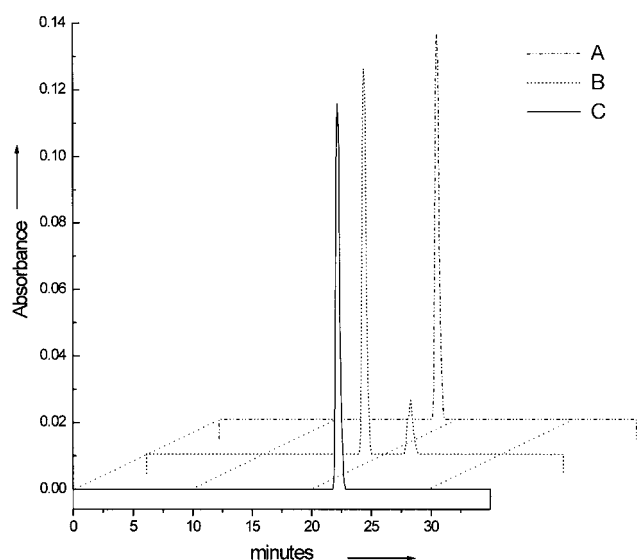


Figure 1. HPLC analysis (UV recording at 450 nm). A: Organic extract of the crude reaction mixture; only one product (**2**) is present. B: Recrystallization solution; formation of a second product (**4**) is observed. C: The green crystals (**4**) isolated from the recrystallization process of **2**.

precipitation, the brown product isolated was characterized and proved to be  $[\text{ReO}((\text{CH}_3\text{CH}_2)_2\text{NHCH}_2\text{CH}_2\text{S})(\text{SC}_6\text{H}_4\text{OCH}_3)_3]$  (**1**) for the  $\text{L}^1\text{H}$  ligand and  $[\text{ReO}(\text{C}_5\text{H}_{10}\text{NHCH}_2\text{CH}_2\text{S})(\text{SC}_6\text{H}_4\text{OCH}_3)_3]$  (**2**), for the  $\text{L}^2\text{H}$  ligand.

During the recrystallization process of **2**, in order to obtain crystals suitable for X-ray studies, a gradual change in the color of the solution was observed. HPLC analysis of this solution revealed the presence of a small amount of an additional complex with a retention time of 22 minutes (Figure 1 trace B). After a series of recrystallizations, green crystals were finally isolated and proven by X-ray analysis to be the  $[\text{ReO}(\text{L}^2)(\text{L})_2]$  product,  $[\text{ReO}(\text{C}_5\text{H}_{10}\text{NCH}_2\text{CH}_2\text{S})(\text{SC}_6\text{H}_4\text{OCH}_3)_2]$  (**4**). HPLC analysis of the crystals of **4** gave the peak at 22 minutes, proving that the crystallized product is the one generated from **2** (Figure 1 trace C). Similarly, HPLC analysis of **1** indicated the existence of a small amount of  $[\text{ReO}((\text{CH}_3\text{CH}_2)_2\text{NCH}_2\text{CH}_2\text{S})(\text{SC}_6\text{H}_4\text{OCH}_3)_2]$  (**3**) at approximately 22 minutes.

Our findings indicate that in solution, the complexes  $[\text{ReO}(\text{L}^n)(\text{L})_3]$ , with three coordinated monothiois, gradually transform into the complexes  $[\text{ReO}(\text{L}^n)(\text{L})_2]$ , with two coordinated monothiois.

Complexes **1**, **2**, and **4** gave correct elemental analyses. Complex **3** was not subjected to elemental analysis, since it was never isolated in pure form. The IR spectra of **1**, **2**, **3**, and **4** exhibit strong  $\text{Re}=\text{O}$  stretching bands at 949, 943, 960, and  $958\text{ cm}^{-1}$  respectively. These values are consistent with those reported for several other well-characterized mono-oxo complexes of rhenium.<sup>[13]</sup> X-ray crystallographic data for **1** and **4** and NMR data for **3** and **4** are presented below.

Complexes **1** and **2** are brown, while **3** and **4** are green. They are slightly soluble in dichloromethane, chloroform, methanol, and ethanol and are insoluble in ether, pentane, and water. They are stable in the solid state for a period of months, and their stability is not affected by the presence of air.

**Synthesis and isolation of  $[\text{ReO}(\text{L}^n)(\text{L})_3]$  and  $[\text{ReO}(\text{L}^n)(\text{L})_2]$  complexes:** The oxotechnetium mixed-ligand complexes were prepared in a similar manner to the oxorhenium complexes by the reaction of the bidentate ligands  $\text{L}^n\text{H}$  ( $n=1$  and  $2$ ) and the monodentate thiol (LH) with  $^{99\text{g}}\text{Tc}$ -gluconate precursor<sup>[14]</sup> in a ratio of  $^{99\text{g}}\text{Tc}$ -precursor/ $\text{L}^n\text{H}$ /LH = 1:1:3. In each case, after extraction of the reaction mixture with dichloromethane, HPLC analysis of the organic phase revealed the presence of two complexes (Figure 2

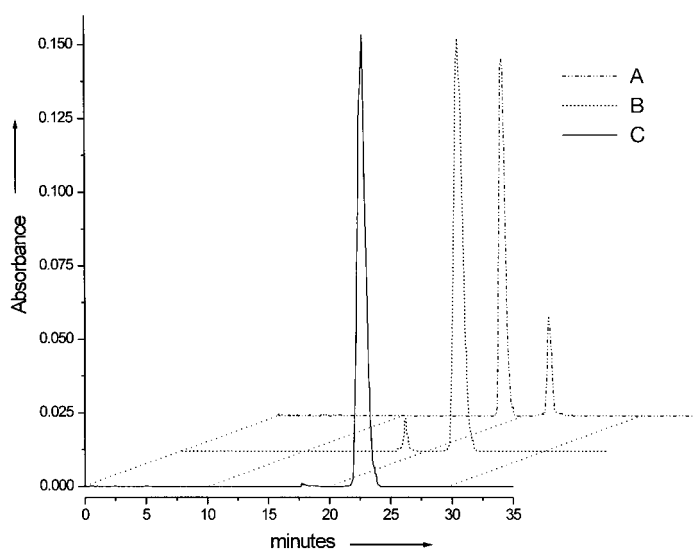


Figure 2. A: HPLC analysis of the crude reaction mixture from the preparation of **5** (organic extract); two complexes, **5** at 18 min and **7** at 22 min, are present. B: HPLC analysis of the above solution three days later; **5** has been converted to **7**. C: HPLC analysis of the crystalline precipitate (complex **7**).

trace A). The major product was eluted at 18 minutes and the minor one at 22 minutes. These retention times were the same as those of the oxorhenium complexes  $[\text{ReO}(\text{L}^n)(\text{L})_3]$  (**1**, **2**) and  $[\text{ReO}(\text{L}^n)(\text{L})_2]$  (**3**, **4**) suggesting the formation of analogous oxotechnetium complexes,  $[\text{ReO}(\text{L}^n)(\text{L})_3]$  (**5**, **6**) and  $[\text{ReO}(\text{L}^n)(\text{L})_2]$  (**7**, **8**). Three days later, HPLC analysis showed that the peak at 22 minutes became the predominant

peak (Figure 2 trace B) indicating a quantitative transformation of complexes **5** and **6** ( $[\text{Re}(\text{L}^n)(\text{L}_3)]$ ) to **7** and **8** ( $[\text{Re}(\text{L}^n)(\text{L}_2)]$ ) respectively. Meanwhile, in each case, a crystalline product precipitated with an HPLC retention time of 22 minutes (Figure 2 trace C). Elemental analysis, X-ray crystallography, and spectroscopic methods confirm that the crystalline complexes were  $[\text{Re}(\text{L}^n)(\text{L}_2)]$  (**7**) in the case of the  $\text{L}^1\text{H}$  and  $[\text{Re}(\text{L}^n)(\text{L}_2)]$  (**8**) in the case of the  $\text{L}^2\text{H}$  ligand. We are once again led to the conclusion that the  $[\text{Re}(\text{L}^n)(\text{L}_3)]$  complexes gradually convert to the  $[\text{Re}(\text{L}^n)(\text{L}_2)]$  complexes. The conversion is much faster in the case of technetium than in the case of rhenium.

The IR spectra of complexes **7** and **8** exhibit strong  $\text{Tc}=\text{O}$  stretching vibrations at 938 and 942  $\text{cm}^{-1}$ , respectively, which is consistent with other values reported for oxotechnetium species.<sup>[15]</sup> The crystallographic data for **7** and NMR data for **7** and **8** are presented below. Even though good quality crystals were obtained for **8**, complete X-ray analysis was not carried out since the calculated unit cell parameters indicated that the complex was isostructural to **4**.

Complexes **7** and **8** are reddish-brown crystalline solids, soluble in dichloromethane and chloroform, slightly soluble in ethanol and methanol, and insoluble in pentane and water. They are stable in the solid state and in solution, as confirmed by HPLC and NMR studies.

**X-ray crystallographic studies of complexes 1, 4, and 7:** ORTEP diagrams of complexes **1**, **4**, and **7** are shown in Figures 3, 4, and 5, respectively, while a summary of crystal data, and selected bond lengths and selected angles are given in Tables 1 and 2, respectively.

In complex **1** the coordination geometry around rhenium is square pyramidal, with four sulfur atoms in the basal plane and the oxo group in the apical position (Figure 3). Three of the four sulfur atoms of the basal plane come from the monodentate thiol ligands, while the fourth belongs to the  $\text{L}^1\text{H}$  bidentate ligand,  $(\text{CH}_3\text{CH}_2)_2\text{NCH}_2\text{CH}_2\text{S}^-$ , which acts as a monodentate ligand, with the nitrogen atom being protonated

Table 1. Summary of crystal data for complexes **1**, **4**, and **7**.

	<b>1</b> · 0.2 $\text{CHCl}_3$	<b>4</b>	<b>7</b> · 0.5 $\text{H}_2\text{O}$
formula	$\text{C}_{27.2}\text{H}_{36.2}\text{Cl}_{0.6}\text{NO}_4\text{ReS}_4$	$\text{C}_{21}\text{H}_{28}\text{NO}_3\text{ReS}_3$	$\text{C}_{20}\text{H}_{29}\text{NO}_{3.5}\text{S}_3\text{Tc}$
$M_r$	776.92	624.82	533.65
$a$ [Å]	12.651(6)	7.990(5)	25.19(2)
$b$ [Å]	13.276(6)	18.091(9)	9.320(6)
$c$ [Å]	20.22(1)	16.302(9)	23.27(1)
$\beta$ [°]	103.34(2)	99.42(2)	118.84(2)
$V$ [Å <sup>3</sup> ]	3304(1)	2324(1)	4786(1)
$Z$	4	4	8
$\rho_{\text{calcd}}$ [g cm <sup>-3</sup> ]	1.562	1.785	1.481
space group	$P2_1/c$	$P2_1/n$	$C2/c$
$T$ [K]	298	298	298
$\mu$ [cm <sup>-1</sup> ]	4.010	5.519	0.886
octants collected	$h, k, \pm l$	$h, k, \pm l$	$\pm h, k, -l$
GOF on $F^2$	1.032	1.158	1.035
$R1$	0.0382 <sup>[a]</sup>	0.0877 <sup>[b]</sup>	0.0539 <sup>[c]</sup>
$wR2$	0.1051 <sup>[a]</sup>	0.2020 <sup>[b]</sup>	0.1228 <sup>[c]</sup>

[a] For 4497 reflections with  $I > 2\sigma(I)$ . [b] For 2669 reflections with  $I > 2\sigma(I)$ . [c] For 2300 reflections with  $I > 2\sigma(I)$ .

Table 2. Selected bond lengths [Å] and angles [°] of complexes **1**, **4**, and **7**.

	Complex <b>1</b>	Complex <b>4</b>	Complex <b>7</b>		
Re–O1	1.689(5)	Re–O1	1.66(2)	Tc–O1	1.659(5)
Re–S1	2.340(2)	Re–N1	2.23(2)	Tc–N1	2.256(7)
Re–S2	2.327(2)	Re–S1	2.287(6)	Tc–S1	2.289(3)
Re–S3	2.335(2)	Re–S2	2.310(5)	Tc–S2	2.329(3)
Re–S4	2.345(2)	Re–S3	2.295(5)	Tc–S3	2.294(3)
O1–Re–S2	109.8(2)	O1–Re–N1	97.6(7)	O1–Tc–N1	105.3(3)
S2–Re–S3	84.3(1)	O1–Re–S1	115.8(6)	O1–Tc–S1	111.3(2)
S2–Re–S1	143.2(1)	N1–Re–S1	81.3(4)	N1–Tc–S1	81.3(2)
O1–Re–S4	107.2(2)	O1–Re–S3	111.8(6)	O1–Tc–S3	106.6(2)
S3–Re–S4	146.7(1)	N1–Re–S3	84.9(4)	N1–Tc–S3	148.1(2)
O1–Re–S3	106.1(2)	S1–Re–S3	131.7(2)	S1–Tc–S3	86.2(1)
O1–Re–S1	106.9(2)	O1–Re–S2	105.9(6)	O1–Tc–S2	110.0(2)
S3–Re–S1	85.4(1)	N1–Re–S2	156.5(5)	N1–Tc–S2	83.3(2)
S2–Re–S4	85.3(1)	S1–Re–S2	87.4(2)	S1–Tc–S2	138.4(1)
S1–Re–S4	84.2(1)	S3–Re–S2	111.1(6)	S3–Tc–S2	87.0(1)

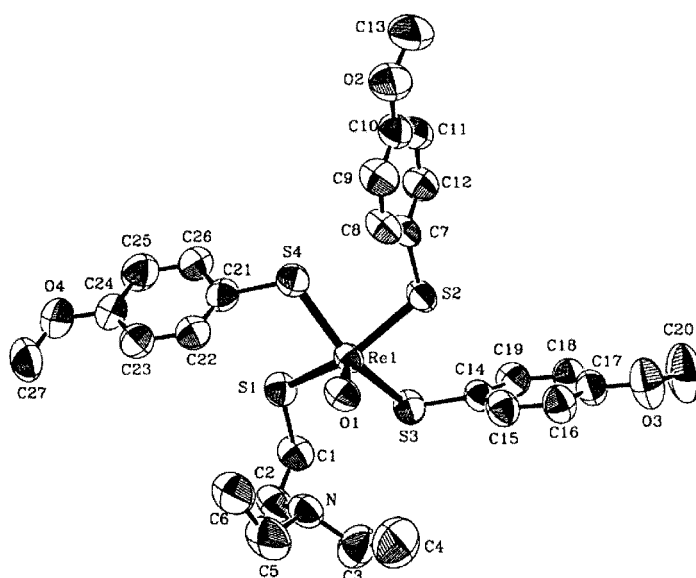


Figure 3. ORTEP diagram of complex **1**.

and hydrogen bonded to the oxo group ( $\text{H} \cdots \text{O1} = 2.48(7)$  Å,  $\text{N} \cdots \text{O1} = 3.429(8)$  Å,  $\text{N}-\text{H} \cdots \text{O} = 154^\circ$ ). The rhenium atom lies 0.70 Å out of the basal plane of the square pyramid toward the double-bonded oxygen. The angles between the opposite atoms of the basal plane ( $\text{S2}-\text{Re}-\text{S1} = 143.24(7)^\circ$  and  $\text{S3}-\text{Re}-\text{S4} = 146.67(8)^\circ$ ) deviate about  $35^\circ$  from the ideal  $180^\circ$ . However, because of their almost equal values, the calculated trigonality index ( $\tau$ ) is 0.06, a value very close to zero, which in turn corresponds to a perfect square pyramid.<sup>[16]</sup> The  $\text{Re}=\text{O}$  (1.689(5) Å) and the  $\text{Re}-\text{S}$  (2.335(2)–2.345(2) Å) bond lengths are in the ranges observed in other analogous complexes.<sup>[7a]</sup>

The coordination requirements of rhenium in **4** are fulfilled by the SN donor atom set of the  $\text{L}^2\text{H}$  bidentate ligand and the two S atoms of the monodentate thiols (Figure 4). These atoms define the equatorial plane of a trigonally distorted square pyramid, with the oxo group in the apical position. The calculated value for the trigonality index,  $\tau = 0.41$ , is intermediate between the theoretical values of zero for a square pyramid and one for a trigonal bipyramid. This is due to the great difference of  $\sim 25^\circ$  between the angles  $\text{N1}-\text{Re}-\text{S2}$  and

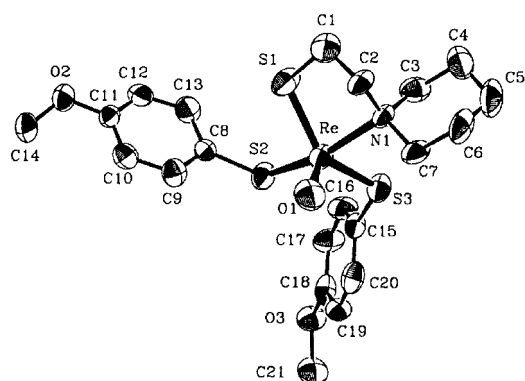


Figure 4. ORTEP diagram of complex 4.

S1–Re–S3 ( $156.5(5)^\circ$  and  $131.7(2)^\circ$  respectively) of the basal plane and their large deviations from the ideal  $180^\circ$ . Rhenium lies  $0.70 \text{ \AA}$  out of the basal plane toward the apical oxo group. The chelating five-membered ring in the coordination sphere adopts the stable envelope configuration with N1 being  $0.77 \text{ \AA}$  out of the mean plane defined by Re, C1, C2, and S1, as is also the case of the technetium analogue presented below. The dihedral angle of the chelating atoms of the ligand (S1–C1–C2–N1) is  $46.9^\circ$ . The Re=O bond length is  $1.66(2) \text{ \AA}$ , similar to the Tc=O bond in the analogous complex 7, which is  $1.659(5) \text{ \AA}$ . The M–N1 (M = Re, Tc in complexes 4 and 7, respectively) bond lengths are  $2.256(7)$  and  $2.23(2) \text{ \AA}$  respectively; these values are slightly longer than usual ( $2.0$ – $2.21 \text{ \AA}$ ),<sup>[17]</sup> but have also been previously observed in analogous rhenium and technetium complexes with trigonally distorted square pyramidal geometry about the metal.<sup>[18]</sup> Finally, the Re–S and Tc–S bond lengths fall in the range of  $2.29$ – $2.32 \text{ \AA}$ , as has been observed in other well-characterized complexes.<sup>[17]</sup>

The coordination geometry about the technetium atom in 7 is square pyramidal with the SN donor-atom set of the ligand and the two S atoms of the monodentate thiols in the basal plane, while the oxo group is in the apical position (Figure 5).

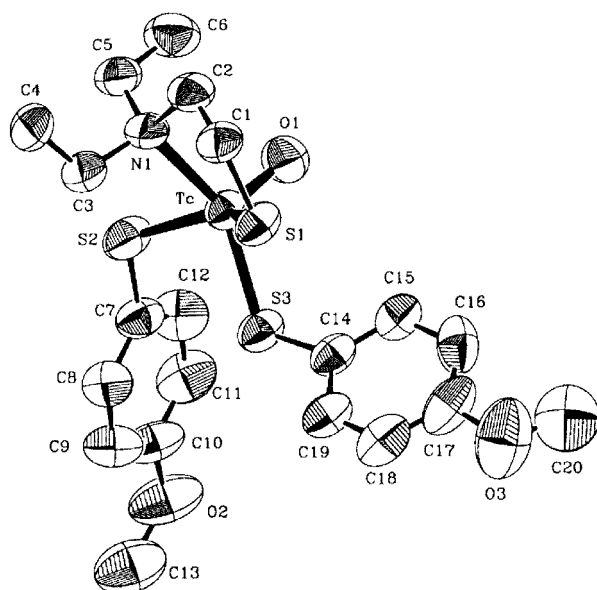


Figure 5. ORTEP diagram of complex 7.

Technetium lies  $0.69 \text{ \AA}$  out of the basal plane toward the oxo group. The angles between the opposite atoms of the basal plane deviate significantly from the ideal value of  $180^\circ$  (N1–Tc–S3 =  $148.1(2)^\circ$  and S1–Tc–S2 =  $138.4(1)^\circ$ ), resulting in the distortion of the square pyramid (calculated trigonality index  $\tau = 0.16$ ). The five-membered ring defined by the metal and the chelating atoms of the ligand exists in the envelope form with N1 being  $0.82 \text{ \AA}$  out of the best mean plane formed by Tc, C1, C2, and S1. The dihedral angle of the chelating atoms S1–C1–C2–N1 of the ligand is  $45.1^\circ$ . The bond lengths in the coordination sphere fall in the ranges observed in analogous complexes.<sup>[17]</sup>

**NMR studies of complexes 3, 4, 7, and 8:** NMR spectra of the  $[\text{ReO}(\text{L}^n)(\text{L})_2]$  (3, 4) and  $[\text{TcO}(\text{L}^n)(\text{L})_2]$  (7, 8) complexes were obtained in  $\text{CDCl}_3$  at  $25^\circ\text{C}$ . Assignments were based on a series of two-dimensional homo- and heterocorrelation spectra.  $^1\text{H}$  and  $^{13}\text{C}$  chemical shifts for 3, 4, 7, and 8 are reported in Tables 3 and 4. Figure 6 displays the  $^1\text{H}$ – $^1\text{H}$  correlation (COSY) spectrum of complex 8. The

Table 3.  $^1\text{H}$  chemical shifts ( $\delta_{\text{H}}$ ) of complexes 3, 4, 7, and 8 in  $\text{CDCl}_3$  at  $25^\circ\text{C}$ . The numbering of the atoms is shown in Scheme 2.

	3	4	7	8
H1 <i>endo</i>	3.13	3.23 <sup>[a]</sup>	3.14	3.22
H1 <i>exo</i>	2.66	2.73	2.75	2.83
H2 <i>endo</i>	3.37 <sup>[a]</sup>	4.42	3.63	4.30
H2 <i>exo</i>	3.37 <sup>[a]</sup>	3.26 <sup>[a]</sup>	3.24 <sup>[a]</sup>	3.57 <sup>[a]</sup>
H3	4.00, 3.45 <sup>[a]</sup>	4.94, 3.78 <sup>[a]</sup>	3.93, 3.44 <sup>[a]</sup>	4.92, 3.88 <sup>[a]</sup>
H4	1.57	2.20, <sup>[a]</sup> 1.77 <sup>[a]</sup>	1.65	2.21, <sup>[a]</sup> 1.81
H5	3.46, <sup>[a]</sup> 2.20	1.97, <sup>[a]</sup> 1.75 <sup>[a]</sup>	3.29, <sup>[a]</sup> 2.12	1.91, <sup>[a]</sup> 1.59 <sup>[a]</sup>
H6	1.23	1.86, <sup>[a]</sup> 1.57 <sup>[a]</sup>	1.22	1.84, <sup>[a]</sup> 1.54 <sup>[a]</sup>
H7	–	3.62, 2.18 <sup>[a]</sup>	–	3.49, 2.13
H2' (H6')	7.49	7.51	7.50	7.53
H3' (H5')	6.91	6.93	6.89	6.90
H7'	3.84	3.84	3.84	3.84
H2'' (H6'')	7.33	7.29	7.33	7.30
H3'' (H5'')	6.85	6.84	6.84	6.82
H7''	3.80	3.80	3.80	3.80

[a] Chemical shifts of overlapping multiplets were defined from the correlation peaks of the two-dimensional NMR experiments.

Table 4.  $^{13}\text{C}$  chemical shifts ( $\delta_{\text{C}}$ ) of complexes 3, 4, 7, and 8 in  $\text{CDCl}_3$  at  $25^\circ\text{C}$ . The numbering of the atoms is shown in Scheme 2.

	3	4	7	8
C1	37.32	38.74	33.69	34.95
C2	64.57	64.87	60.49	60.78
C3	54.06	64.70	52.77	63.77
C4	11.84	22.35	11.73	21.91
C5	51.33	22.91	50.58	23.21
C6	7.82	19.72	7.63	19.62
C7	–	52.56	–	52.03
C1'	143.96	144.62	139.38	139.83
C2' (C-6')	135.97	135.96	136.62	136.59
C3' (C-5')	113.64	113.68	113.65	113.68
C4'	159.25	159.30	159.29	159.33
C7'	55.22	55.22	55.23	55.23
C1''	<sup>[a]</sup>	131.96	128.92	128.71
C2'' (C6'')	134.82	134.80	135.32	135.30
C3'' (C5'')	113.28	113.29	113.18	113.15
C4''	158.48	158.28	158.60	158.55
C7''	55.17	55.16	55.18	55.17

[a] Peak hidden under others.

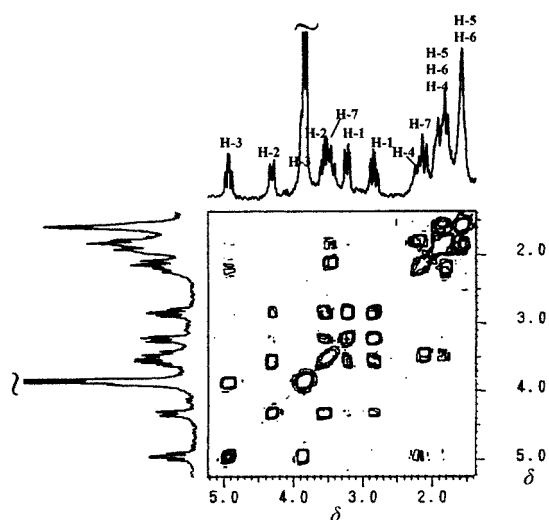


Figure 6.  $^1\text{H}$ - $^1\text{H}$  correlation spectrum of complex **8** (range 5.2–1.4 ppm) in  $\text{CDCl}_3$ .

$[\text{ReO}(\text{L}^n)(\text{L})_3]$  complexes in  $\text{CDCl}_3$  gave bunched-up spectra of low resolution, as can be seen in Figure 7 (bottom spectrum) for complex **1**. Detailed NMR assignments were not feasible for these complexes.

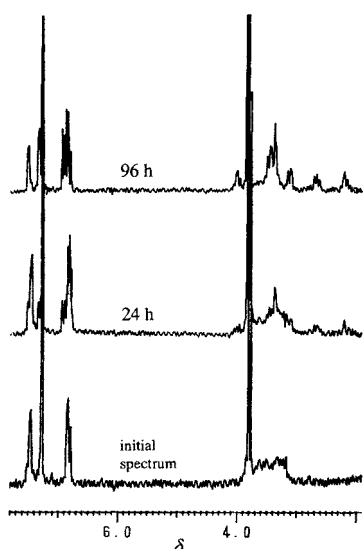


Figure 7. Monitoring the transformation of complex **1** to complex **3** by NMR spectroscopy.

The NMR spectra of **3**, **4**, **7**, and **8** displayed the basic characteristics of the aminothiols complexes observed in our previous studies.<sup>[8, 18, 19]</sup> Specifically: All geminal protons of the aminothiol ligand, being diastereotopic, exhibit distinct chemical shifts. Protons of the S–C1–C2–N part, being on the same side as the oxygen of the oxometal core (*endo* protons), generally appear downfield relative to those on the opposite side (*exo* protons) with  $\Delta\delta$  reaching up to 1.2 ppm in these types of complexes. Differentiation in chemical shift is also observed between symmetric protons and carbons of the diethyl or piperidinyll substituents of nitrogen. Substituents closer to the oxygen of the oxometal core (*syn* substituents) appear to be deshielded relative to those on the opposite side

(*anti* substituents). For example, carbons C3 and C4 of the *syn* ethyl group in complexes **3** and **7** appear downfield by 2–4 ppm relative to C5 and C6 of the *anti* ethyl group. Correspondingly, in complexes **4** and **8**, carbons C3 and C4 of the piperidinyll substituent appear downfield by 12–13 ppm relative to C7 and C6.

The chemical shifts of the protons essentially are not different in analogous rhenium and technetium complexes. In contrast, the chemical shifts of carbons close to the metal center show metal dependence. Specifically, carbons coordinated to rhenium through sulfur (carbons C1, C1', C1'') appear downfield by 3–4 ppm relative to their technetium analogues. For carbons coordinated to rhenium through nitrogen (C2, C3, C5 in complexes **3** and **7** and C2, C3, C7 in complexes **4** and **8**) the difference ranges from 0.5–4 ppm.

Because of the asymmetry of the molecules, the two aromatic *p*-methoxythiophenol substituents are in different magnetic environments and appear at different chemical shifts. Distinction of the absolute position of each of the aromatic substituents was not possible from the NMR data, and the chemical shifts reported in Tables 3 and 4 are not position specific.

The transformation of the  $[\text{ReO}(\text{L}^n)(\text{L})_3]$  complexes **1** and **2** to the  $[\text{ReO}(\text{L}^n)(\text{L})_2]$  complexes **3** and **4** was followed by NMR spectroscopy. Complexes **1** and **2** were dissolved in  $\text{CDCl}_3$ , and spectra of the solutions were periodically obtained (Figure 7). In the methoxy and aromatic proton region new peaks appeared at  $\delta_{\text{H}} = 3.79$ , 6.81 and 7.28, belonging to free *p*-methoxythiophenol. In the aminothiols proton region the resonances originally present were replaced by others corresponding to the  $[\text{ReO}(\text{L}^n)(\text{L})_2]$  complexes as proven by comparison of the NMR spectra with the chemical shifts of the isolated crystalline  $[\text{ReO}(\text{L}^2)(\text{L})_2]$  complex **4** as well as with the  $[\text{99m}\text{TcO}(\text{L}^n)(\text{L})_2]$  complexes **7** and **8**.

**Synthesis of  $^{99\text{m}}\text{Tc}$  tracer complexes:** The mixed-ligand complexes with  $^{99\text{m}}\text{Tc}$  were prepared by using equimolar quantities of the ligands L<sup>1</sup>H and LH ranging from 2 nmol to 20  $\mu\text{mol}$  and  $^{99\text{m}}\text{Tc}$ -glucoheptonate as the precursor (Table 5). The complexes were extracted from the reaction mixture with dichloromethane. When 2 nmol of the ligands were used, the labeling yield was 5% as calculated by organic solvent extraction of the aqueous reaction mixture. By increasing the quantities of the ligands to 20 nmol we improved the labeling yield to 50%. HPLC analysis of the extracted fraction showed the formation of two complexes (Figure 8 trace A). The minor peak (20%) had a retention time of 18 minutes, which was similar to that of the oxotechnetium

Table 5. Percentage yield of complexes **9** and **11** for different quantities of  $(\text{CH}_3\text{CH}_2)_2\text{NCH}_2\text{CH}_2\text{SH}$  (L<sup>1</sup>H) and *p*- $\text{CH}_3\text{OC}_6\text{H}_4\text{SH}$  (LH) ligands used.

L <sup>1</sup> H	LH	Extraction yield	Percentage of complex <b>9</b>	Percentage of complex <b>11</b>
20 $\mu\text{mol}$	20 $\mu\text{mol}$	> 80%	93	7
2 $\mu\text{mol}$	2 $\mu\text{mol}$	80%	53	47
200 nmol	200 nmol	80%	27	73
20 nmol	20 nmol	50%	20	80
2 nmol	2 nmol	< 5%	–	–

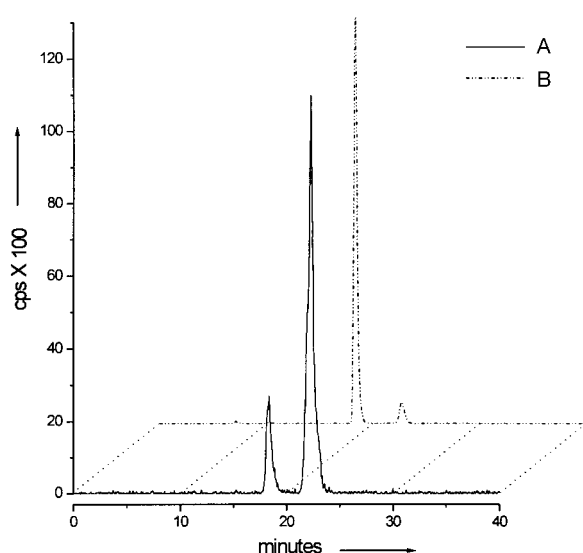


Figure 8. HPLC analysis, radiochromatogram, of the organic extract of the preparation mixture of the complexes at the technetium tracer level ( $^{99m}\text{Tc}$ ) using 20 nmol ligand (A), and 20  $\mu\text{mol}$  ligand (B).

$^{99g}\text{TcO}(\text{L}^1)(\text{L}_2)_2$  complex (**5**) and of the oxorhenium  $[\text{ReO}(\text{L}^1)(\text{L}_2)_2]$  complex (**1**), suggesting the formation of the  $^{99m}\text{TcO}(\text{L}^1)(\text{L}_2)_2$  complex (**9**). The major peak (80%) had a retention time of 22 minutes, the same as that of  $^{99g}\text{TcO}(\text{L}^1)(\text{L}_2)_2$  (**7**), indicating that complex  $^{99m}\text{TcO}(\text{L}^1)(\text{L}_2)_2$  (**11**) is also formed at the tracer level.

The labeling yield was improved to 80% by increasing the amount of ligand to 200 nmol. HPLC analysis of the organic extract showed a slight decrease in the percentage of **11** (73%). Further increase of the quantities of the ligands to 2  $\mu\text{mol}$  or 20  $\mu\text{mol}$  did not enhance the labeling yield, but had a strong effect on the composition of the reaction mixture. At a concentration of 2  $\mu\text{mol}$  the two complexes were in a ratio of about 1:1. When the concentration of the ligands was 20  $\mu\text{mol}$ , complex **9** became the predominant product of the reaction at 93% yield (Figure 8 trace B). When complex **9** was isolated and analyzed by HPLC after 30 minutes, 24% of it was converted to complex **11**. Four hours after isolation, 80% of **9** was converted to **11**. Apparently, isolation of **9** from its thiol-rich environment enhances its transformation into **11**. In

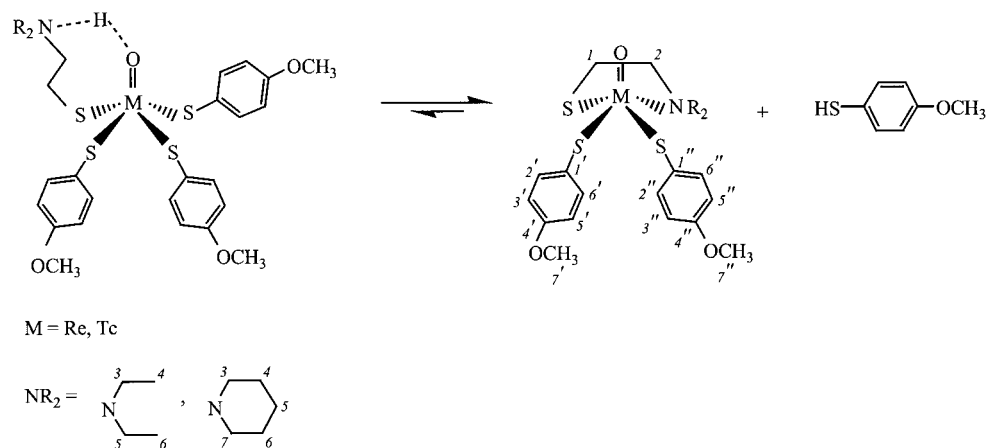
contrast, HPLC analysis of isolated complex **11** showed that it is stable in solution for at least six hours. The same results were obtained when the bidentate aminothiol  $\text{L}^2\text{H}$  was used.

## Discussion

Our experimental evidence suggests that interaction of the  $\text{M}^{\text{VO}}$  ( $\text{M} = ^{99g}\text{Tc}$  or  $\text{Re}$ ) precursors with the bidentate aminothiol ligand  $\text{L}^n\text{H}$  and the monothiol  $\text{LH}$  in ratio of 1:1:3 leads to initial formation of the  $[\text{MO}(\text{L}^n)(\text{L}_2)_2]$  type of complex. It is important to note that  $[\text{MO}(\text{L}^n)(\text{L}_2)_2]$  is formed even when the monothiol  $\text{LH}$  ligand is present at the lower ratio of 1:1:1.

The  $[\text{MO}(\text{L}^n)(\text{L}_2)_2]$  complexes are of the  $[\text{S}][\text{S}]_3$  type with four deprotonated thiols coordinated to the metal. The overall charge of the complexes is zero because the nitrogen of the  $\text{L}^n\text{H}$  aminothiol ligand is protonated and hydrogen-bonded to the oxygen of the  $\text{M}=\text{O}$  core.

The  $[\text{MO}(\text{L}^n)(\text{L}_2)_2]$  complexes subsequently convert to  $[\text{MO}(\text{L}^n)(\text{L}_2)]$  complexes, with the coordination of the nitrogen atom of the aminothiol ligand and the expulsion of one monothiol (Scheme 2) as evidenced by HPLC and NMR spectroscopy. This conversion is a ligand substitution process on the metal center and is expected to be faster for technetium than for rhenium because of smaller ligand field splittings in the former metal.<sup>[2b]</sup> A number of examples in the literature confirm this trend with the reported rate ratio  $k^{\text{Tc}}/k^{\text{Re}}$  ranging from about 60 for the rate of unimolecular racemization of  $\text{M}^{\text{V}}$  penicillamine complexes<sup>[20]</sup> to about  $10^4$  for the bimolecular exchange of pyridine in cationic  $\text{trans-}[\text{M}(\text{O})_2(\text{py})_4]^+$  complexes in nitromethane.<sup>[2b]</sup> Our findings for the transformation of  $[\text{MO}(\text{L}^n)(\text{L}_2)_2]$  to  $[\text{MO}(\text{L}^n)(\text{L}_2)]$  are in agreement with existing data in the literature, since the oxotechnetium complexes **5** and **6** transform to the stable **7** and **8** much faster than their oxorhenium analogues. As a result, in the oxorhenium case only one complex at 18 minutes,  $[\text{ReO}(\text{L}^n)(\text{L}_2)_2]$ , is present in the HPLC chromatogram of the reaction mixture (Figure 1 trace A). On the other hand, in the oxotechnetium case the second complex at 22 minutes is always present both in  $^{99g}\text{Tc}$  as well as in  $^{99m}\text{Tc}$  preparations (Figures 2 and 8). Owing to the faster conversion of



Scheme 2. Transformation of  $[\text{MO}(\text{L}^n)(\text{L}_2)_2]$  to  $[\text{MO}(\text{L}^n)(\text{L}_2)]$  and numbering for the NMR studies.

[<sup>99g</sup>TcO(L<sup>n</sup>)(L<sub>3</sub>)] to [<sup>99g</sup>TcO(L<sup>n</sup>)(L<sub>2</sub>)] it was not possible to isolate the [<sup>99g</sup>TcO(L<sup>n</sup>)(L<sub>3</sub>)] complexes.

The [MO(L<sup>n</sup>)(L<sub>2</sub>)] complexes of [NS][S][S] type are neutral and lipophilic. Complexes prepared at the carrier level (Re, <sup>99g</sup>Tc) are stable in the solid state and also in chloroform for a period of months. At the tracer level, the [<sup>99m</sup>TcO(L<sup>n</sup>)(L<sub>2</sub>)] complexes remain stable in dichloromethane and aqueous-methanolic solutions for a six hour period (typical for radiopharmaceutical applications of <sup>99m</sup>Tc), during which checks were performed periodically with HPLC.

The transformation of [MO(L<sup>n</sup>)(L<sub>3</sub>)] to [MO(L<sup>n</sup>)(L<sub>2</sub>)] appears to be a reversible process, since its rate is greatly affected by the presence of the monothiol ligand. Removal of the product [MO(L<sup>n</sup>)(L<sub>3</sub>)] from the reaction mixture for isolation and crystallization purposes speeded up its transformation to the [MO(L<sup>n</sup>)(L<sub>2</sub>)] complex. Apparently, the lack of thiol shifts the equilibrium in Scheme 2 to the right. The reversibility of the reaction was confirmed when an excess of *p*-methoxythiophenol was added in a solution of **7** and **8** in chloroform, and the complexes converted almost quantitatively to **5** and **6** respectively, as witnessed by HPLC.

This existing equilibrium [MO(L<sup>n</sup>)(L<sub>3</sub>)] ⇌ [MO(L<sup>n</sup>)(L<sub>2</sub>)] can explain the varying percentages of complexes [<sup>99m</sup>TcO(L<sup>1</sup>)(L<sub>3</sub>)] (**9**) and [<sup>99m</sup>TcO(L<sup>1</sup>)(L<sub>2</sub>)] (**11**), summarized in Table 5, when different quantities of ligands are used during the synthesis of the oxotechnetium-99m complexes. When 200 nmol of each ligand are used, the excess of *p*-methoxythiophenol is not high enough, the equilibrium shifts to the right, and as a result most of the initially formed [<sup>99m</sup>TcO(L<sup>n</sup>)(L<sub>3</sub>)] converts to [<sup>99m</sup>TcO(L<sup>n</sup>)(L<sub>2</sub>)]. When 20 μmol of each ligand are used, the high excess of *p*-methoxythiophenol present prevents the fast conversion of [<sup>99m</sup>TcO(L<sup>n</sup>)(L<sub>3</sub>)] to [<sup>99m</sup>TcO(L<sup>n</sup>)(L<sub>2</sub>)].

Our investigations on the relative yields of the oxotechnetium-99m complexes, [<sup>99m</sup>TcO(L<sup>n</sup>)(L<sub>3</sub>)] and [<sup>99m</sup>TcO(L<sup>n</sup>)(L<sub>2</sub>)], with varying ligand concentrations led to useful information from the radiopharmaceutical point of view. Specifically, the finding that the stable product [<sup>99m</sup>TcO(L<sup>n</sup>)(L<sub>2</sub>)] is preferentially formed at low concentration of ligands is an important factor in the preparation of <sup>99m</sup>Tc radiopharmaceuticals, for which low concentrations of ligands are required.<sup>[1c]</sup> Data obtained so far provide a solid foundation for the development of potential diagnostic (<sup>99m</sup>Tc) or therapeutic (<sup>186</sup>Re or <sup>188</sup>Re) radiopharmaceuticals using the [NS][S][S] mixed ligand system.

## Experimental Section

**General:** Caution!!! Technetium-99 is a weak β-emitter (0.292 MeV) with a half-life of 2.12 × 10<sup>5</sup> years. All manipulations of solutions and solids were carried out in a laboratory approved for the handling of low-level radioisotopes. Normal safety procedures were followed at all times to prevent contamination. Technetium-99m is a gamma-emitter (141 keV) with a half-life of 6 h. Handling of solutions containing this radionuclide always proceeded behind sufficient lead shielding.

IR spectra were recorded as KBr pellets in the 4000–500 cm<sup>-1</sup> range on a Perkin–Elmer 1600 FT-IR spectrophotometer and were referenced to polystyrene. <sup>1</sup>H (250.13 MHz) and <sup>13</sup>C (62.90 MHz) NMR spectra were recorded in CDCl<sub>3</sub> (Aldrich) on a Bruker AC250E spectrometer equipped with an Aspect 3000 Computer. Chemical shifts (δ, ppm) were referenced

to TMS. Parameters for the two-dimensional experiments (COSY, HETCOR, NOESY, etc.) have been previously reported.<sup>[8, 15, 19]</sup> Elemental analyses were performed on a Perkin–Elmer 2400/II automatic analyzer.

<sup>99g</sup>Tc was purchased as ammonium pertechnetate from the Oak Ridge National Laboratory. The impure black solid was purified prior to its use by treatment overnight with hydrogen peroxide and ammonium hydroxide in methanol. Evaporation of the solvent gave ammonium pertechnetate as a white powder. Na<sup>99m</sup>TcO<sub>4</sub> was obtained in physiological saline as commercial <sup>99m</sup>Mo/<sup>99m</sup>Tc-generator eluate (Cis International). All laboratory chemicals were reagent grade. The *p*-methoxythiophenol used as coligand was purchased from Fluka. The bidentate ligands were synthesized according to the literature,<sup>[9]</sup> as were the rhenium precursors [ReOCl<sub>3</sub>(PPh<sub>3</sub>)<sub>2</sub>]<sup>[10]</sup> and rhenium gluconate.<sup>[11]</sup> The rhenium precursor oxorhenium citrate was generated in situ by a known method.<sup>[12]</sup>

High-performance liquid chromatography (HPLC) was conducted on a Waters 600 Millennium Chromatography System coupled to both a Waters 991 photodiode array detector (UV trace for <sup>99g</sup>Tc, Re, and ligands) and a GABI gamma detector from Raytest (γ trace for <sup>99m</sup>Tc). Separations were achieved on a C18 RP column eluted with a binary gradient system at a 1.0 mL min<sup>-1</sup> flow rate. Mobile phase A consisted of MeOH, while mobile phase B was H<sub>2</sub>O. The elution profile was: 0–10 min isocratic with 50% A; 10–25 min, linear gradient to 80% A; 25–27 min linear gradient to 95% A; 27–32 min isocratic with 95% A. The column was re-equilibrated for 10 min prior to the next injection. Solvents used in chromatographic analysis were HPLC grade.

### Synthesis of [ReO{(C<sub>2</sub>H<sub>5</sub>)<sub>2</sub>NHCH<sub>2</sub>CH<sub>2</sub>S}(SC<sub>6</sub>H<sub>4</sub>OCH<sub>3</sub>)<sub>3</sub>] (**1**):

**Method A, from [ReOCl<sub>3</sub>(PPh<sub>3</sub>)<sub>2</sub>]:** CH<sub>3</sub>COONa in methanol (1M, 2 mL) was added to a stirred suspension of trichlorobis(triphenylphosphane)rhenium(v) oxide (166.6 mg, 0.2 mmol) in methanol (10 mL). A mixture of *N*-(2-mercaptoethyl)diethylamine (L<sup>1</sup>H) (26.6 mg, 0.2 mmol) and *p*-methoxythiophenol (LH) (84 mg, 0.6 mmol) was added under stirring. The reactants were in a 1:1:3 molar ratio and were heated under reflux for approximately 1 h, after which the solution had turned to a dark brown color. After the mixture had cooled to room temperature, CH<sub>2</sub>Cl<sub>2</sub> was added and the organic layer was washed with H<sub>2</sub>O. The organic extract was dried over MgSO<sub>4</sub>, the volume of the solution was reduced to 10 mL, and then methanol (2–3 mL) was added. Slow evaporation of the solvents at room temperature afforded the product of the reaction, [ReO{(C<sub>2</sub>H<sub>5</sub>)<sub>2</sub>NHCH<sub>2</sub>CH<sub>2</sub>S}(SC<sub>6</sub>H<sub>4</sub>OCH<sub>3</sub>)<sub>3</sub>], as brown crystals (70% yield). Crystals suitable for X-ray crystallography were obtained by recrystallization from MeOH/CHCl<sub>3</sub> and slow evaporation. *R*<sub>f</sub> = 0.5 (silica gel, benzene/CHCl<sub>3</sub>/CH<sub>3</sub>CN 50:25:25); IR (KBr pellet):  $\tilde{\nu}$  = 3100 (N–H), 949 (Re=O), 825 cm<sup>-1</sup> (CH–CH, aromatic); elemental analysis calcd (%) for C<sub>27</sub>H<sub>36</sub>NO<sub>4</sub>S<sub>4</sub>Re (753.1): C 43.02, H 4.82, N 1.86, S 16.98; found C 42.31, H 4.75, N 1.68, S 16.93.

**Method B, from rhenium(v) gluconate:** The rhenium(v) gluconate precursor was prepared according to literature.<sup>[11]</sup> Solutions of L<sup>1</sup>H (13.3 mg, 0.1 mmol) and LH (42 mg, 0.3 mmol) in methanol (1 mL each) were mixed and added to a stirred solution of rhenium gluconate (1.45 mL, 0.1 mmol). A brown, mudlike suspension formed instantly. A small quantity of CH<sub>2</sub>Cl<sub>2</sub> was added, and the stirring was continued for a few minutes. A further amount of CH<sub>2</sub>Cl<sub>2</sub> was added, and the mixture was extracted. The organic phase was dried with MgSO<sub>4</sub>, filtered, and MeOH (3–5 mL) was added. A brown product was precipitated by slow evaporation of the above solution (60% yield). *R*<sub>f</sub> = 0.5 (silica gel, benzene/CHCl<sub>3</sub>/CH<sub>3</sub>CN 50:25:25); IR (KBr pellet):  $\tilde{\nu}$  = 3097 (N–H), 948 (Re=O), 824 cm<sup>-1</sup> (CH–CH, aromatic).

**Method C, from oxorhenium citrate:** KReO<sub>4</sub> (57.8 mg, 0.2 mmol) was added to a solution of SnCl<sub>2</sub> (38.9 mg, 0.2 mmol) in citric acid (0.5 M, 5 mL). L<sup>1</sup>H (26.6 mg, 0.2 mmol) and LH (84 mg, 0.6 mmol), each in dichloromethane (4 mL), were added to this mixture simultaneously and in a dropwise fashion. The mixture was stirred at room temperature for 30 min. The pH was adjusted to 9 with 0.5 M NaOH, and the mixture was extracted with CH<sub>2</sub>Cl<sub>2</sub>. Brown crystals were isolated from CH<sub>2</sub>Cl<sub>2</sub>/MeOH solution (60% yield). *R*<sub>f</sub> = 0.5 (silica gel, benzene/CHCl<sub>3</sub>/CH<sub>3</sub>CN 50:25:25); IR (KBr pellet):  $\tilde{\nu}$  = 3100 (N–H), 948 (Re=O), 824 cm<sup>-1</sup> (CH–CH, aromatic).

**Synthesis of [ReO{C<sub>5</sub>H<sub>10</sub>NHCH<sub>2</sub>CH<sub>2</sub>S}(SC<sub>6</sub>H<sub>4</sub>OCH<sub>3</sub>)<sub>3</sub>] (**2**):** The above mentioned procedures (Methods A–C) were followed, but this time *N*-(2-mercaptoethyl)piperidine (L<sup>2</sup>H) (29 mg, 0.2 mmol) was used instead of *N*-(2-mercaptoethyl)diethylamine. Compound **2** was isolated as brown crystals.



**Method A, from [ReOCl<sub>3</sub>(PPh<sub>3</sub>)<sub>2</sub>]:** Yield: 75%;  $R_f = 0.5$  (silica gel, benzene/CHCl<sub>3</sub>/CH<sub>3</sub>CN 50:25:25); IR (KBr pellet):  $\tilde{\nu} = 3096$  (N–H), 943 (Re=O), 823 cm<sup>-1</sup> (CH–CH, aromatic); elemental analysis calcd (%) for C<sub>28</sub>H<sub>26</sub>NO<sub>4</sub>S<sub>2</sub>Re (765.1): C 43.96, H 4.74, N 1.83, S 16.76; found C 44.15, H 4.86, N 1.97, S 17.39.

**Method B, from rhenium(v) gluconate:** Yield: 65%;  $R_f = 0.5$  (silica gel, benzene/CHCl<sub>3</sub>/CH<sub>3</sub>CN 50:25:25); IR (KBr pellet):  $\tilde{\nu} = 3094$  (N–H), 942 (Re=O), 823 cm<sup>-1</sup> (CH–CH, aromatic).

**Method C, from oxorhenium citrate:** Yield: 58%;  $R_f = 0.5$  (silica gel, benzene/CHCl<sub>3</sub>/CH<sub>3</sub>CN 50:25:25); IR (KBr pellet):  $\tilde{\nu} = 3091$  (N–H), 943 (Re=O), 823 cm<sup>-1</sup> (CH–CH, aromatic).

**Isolation of [ReO(C<sub>2</sub>H<sub>10</sub>NCH<sub>2</sub>CH<sub>2</sub>S)(SC<sub>6</sub>H<sub>4</sub>OCH<sub>3</sub>)<sub>2</sub>] (4):** Upon dissolution of the brown crystals of complex **2** in CH<sub>2</sub>Cl<sub>2</sub> or CHCl<sub>3</sub>, a color transition was observed. The initially brown solution turned green. TLC monitoring of the composition of the solution showed the transformation of the initial, single brown product into two different products, a green one and a brown one, with different retention factors. Fractional recrystallization yielded green crystals suitable for X-ray studies in 25% yield.  $R_f = 0.7$  (silica gel, benzene/CHCl<sub>3</sub>/CH<sub>3</sub>CN 50:25:25); IR (KBr pellet):  $\tilde{\nu} = 956$  (Re=O), 817 cm<sup>-1</sup> (CH–CH, aromatic); elemental analysis calcd (%) for C<sub>21</sub>H<sub>28</sub>NO<sub>3</sub>S<sub>3</sub>Re (624.8): C 40.37, H 4.52, N 2.24, S 15.39; found C 40.16, H 4.74, N 2.09, S 15.04.

**Synthesis of [<sup>99m</sup>TcO{(CH<sub>2</sub>CH<sub>2</sub>)<sub>2</sub>NCH<sub>2</sub>CH<sub>2</sub>S}(p-CH<sub>3</sub>OC<sub>6</sub>H<sub>4</sub>)<sub>2</sub>] (7):** A solution of stannous chloride (45 mg, 0.24 mmol) in HCl (1M, 1.0 mL) was added to an aqueous solution of [NH<sub>4</sub>]<sup>99m</sup>TcO<sub>4</sub> (36.2 mg, 0.2 mmol) containing <sup>99m</sup>TcO<sub>4</sub><sup>-</sup> (0.1 mL, 0.5 mCi) and sodium gluconate (200 mg) to obtain the <sup>99m</sup>technetium gluconate precursor. The pH of the solution was adjusted to 7.5 with NaOH (1M). This solution was added, under constant stirring, to a mixture of L<sup>1</sup>H (26.6 mg, 0.2 mmol) and LH (84 mg, 0.6 mmol) in a small amount of methanol. The solution was stirred for 20 min and then extracted twice with dichloromethane. The organic phase was dried over MgSO<sub>4</sub> and filtered. The volume of the solution was reduced to 5 mL and, after the addition of methanol (5 mL), was left at room temperature. Slow evaporation of the solvents afforded the product as red-brown crystals, suitable for X-ray crystal structure determination (70% yield).  $R_f = 0.7$  (silica gel, benzene/CHCl<sub>3</sub>/CH<sub>3</sub>CN 50:25:25); IR (KBr pellet):  $\tilde{\nu} = 938$  (Tc=O), 824 cm<sup>-1</sup> (CH–CH, aromatic); elemental analysis calcd (%) for C<sub>20</sub>H<sub>28</sub>NO<sub>3</sub>S<sub>3</sub>Tc (524.6): C 45.79, H 5.38, N 2.67, S 18.33; found C 45.53, H 5.59, N 2.35, S 17.99.

**Synthesis of [<sup>99m</sup>TcO(C<sub>2</sub>H<sub>10</sub>NCH<sub>2</sub>CH<sub>2</sub>S)(p-CH<sub>3</sub>OC<sub>6</sub>H<sub>4</sub>)<sub>2</sub>] (8):** The same procedure was repeated, this time using *N*-(2-mercaptoethyl)piperidine (29 mg, 0.2 mmol) as the bidentate ligand, L<sup>2</sup>H. Red-brown crystals of complex **8** were isolated (78% yield).  $R_f = 0.7$  (silica gel, benzene/CHCl<sub>3</sub>/CH<sub>3</sub>CN 50:25:25); IR (KBr pellet):  $\tilde{\nu} = 942$  (Tc=O), 821 cm<sup>-1</sup> (CH–CH, aromatic); elemental analysis calcd (%) for C<sub>21</sub>H<sub>28</sub>NO<sub>3</sub>S<sub>3</sub>Tc (536.6): C 47.00, H 5.26, N 2.61, S 17.92; found C 47.23, H 5.09, N 2.78, S 18.03.

**Synthesis of <sup>99m</sup>Tc complexes:** A Gluco/Demoscan kit was reconstituted with 10 mL saline and then a 1.0 mL aliquot was mixed with 0.5–1.0 mL of <sup>99m</sup>Tc-pertechnetate solution (5–10 mCi). The oxotechnetium-99m(v) glucoheptonate solution was added to a centrifuge tube containing equimolar quantities (20 μmol) of the bidentate ligand (L<sup>1</sup>H) and the monodentate ligand (LH) dissolved in 0.2 mL methanol. The mixture was agitated in a vortex mixer and left to react at room temperature for 10 min. The complexes were extracted with CH<sub>2</sub>Cl<sub>2</sub> (3 × 1.5 mL) and the combined organic extracts were dried over MgSO<sub>4</sub> and filtered. The extraction was nearly quantitative. In order to investigate the effect of ligand concentration on radiochemical yield and purity, different quantities of ligands were used in the same procedure. In all cases the organic extracts were analyzed by HPLC in order to characterize the complexes. The results are summarized in Table 5.

**X-ray crystal structure determinations for compounds 1, 4, and 7:** Diffraction measurements were performed on a Crystal Logic Dual Goniometer diffractometer with graphite monochromated MoK<sub>α</sub> radiation ( $\lambda = 0.710730$ ). Unit-cell dimensions were determined and refined by using the angular settings of 25 automatically centered reflections and they appear in Table 1. Intensity data were recorded using a  $\theta - 2\theta$  scan. Three standard reflections monitored every 97 reflections showed less than 3% variation and no decay. Lorentz, polarization, and psi-scan absorption corrections were applied by using Crystal Logic software. The structures

were solved by direct methods by using SHELXS-86<sup>[21]</sup> and refined by full-matrix least-squares techniques on  $F^2$  with SHELXL-93.<sup>[22]</sup>

**Compound 1:**  $2\theta_{\max} = 50^\circ$ , scan speed 2.2° min<sup>-1</sup>, scan range 2.5+ $\alpha_1\alpha_2$  separation, reflections collected/unique/used = 6076/5796 ( $R_{\text{int}} = 0.0158$ )/5796, 417 parameters refined,  $R1/wR2$  (for all data) = 0.0547/0.1189,  $\Delta\rho_{\text{min}}/\Delta\rho_{\text{max}} = 0.830/-0.575$  e Å<sup>-3</sup>,  $\Delta\sigma = 0.312$ . All hydrogen atoms of the methylene and methyl groups were introduced at calculated positions as riding on bonded atoms; the rest were located by difference maps and were refined isotropically. All non-hydrogen atoms were refined anisotropically except those of the solvate chloroform, which were refined isotropically with occupation factors at 0.20.

**Compound 4:**  $2\theta_{\max} = 48^\circ$ , scan speed 0.8° min<sup>-1</sup>, scan range 2.3+ $\alpha_1\alpha_2$  separation, reflections collected/unique/used = 3837/3538 ( $R_{\text{int}} = 0.0701$ )/3532, 293 parameters refined,  $R1/wR2$  (for all data) = 0.1185/0.2284,  $\Delta\rho_{\text{min}}/\Delta\rho_{\text{max}} = 0.925/-0.794$  e Å<sup>-3</sup>,  $\Delta\sigma = 0.010$ . All hydrogen atoms were introduced at calculated positions as riding on bonded atoms except those on C2, C7, and C20, which were located by difference maps and were refined isotropically, while all non-hydrogen atoms were refined anisotropically.

**Compound 7:**  $2\theta_{\max} = 44^\circ$ , scan speed 2.0° min<sup>-1</sup>, scan range 2.4+ $\alpha_1\alpha_2$  separation, reflections collected/unique/used = 3033/2938 ( $R_{\text{int}} = 0.0255$ )/2938, 349 parameters refined,  $R1/wR2$  (for all data) = 0.0734/0.1377,  $\Delta\rho_{\text{min}}/\Delta\rho_{\text{max}} = 0.966/-0.621$  e Å<sup>-3</sup>,  $\Delta\sigma = 0.002$ . All hydrogen atoms (except those of the methyl groups, which were introduced at calculated positions as riding on bonded atoms) were located by difference maps and were refined isotropically, while all non-hydrogen atoms were refined anisotropically.

Crystallographic data (excluding structure factors) for the structures reported in this paper have been deposited with the Cambridge Crystallographic Data Centre as supplementary publication no. CCDC-152000, CCDC-152001, and CCDC-152002. Copies of the data can be obtained free of charge on application to CCDC, 12 Union Road, Cambridge CB2 1EZ, UK (fax: (+44) 1223-336-033; e-mail: deposit@ccdc.cam.ac.uk).

- [1] a) K. Schwochau, *Angew. Chem.* **1994**, *106*, 2349–2358; *Angew. Chem. Int. Ed. Engl.* **1994**, *33*, 2258–2267; b) S. Jurisson, J. Lyndon, *Chem. Rev.* **1999**, *99*, 2205–2218; c) S. Liu, S. Edwards, *Chem. Rev.* **1999**, *99*, 2235–2268; d) A. Duatti in *Technetium, Rhenium and Other Metals in Chemistry and Nuclear Medicine*, Vol. 5 (Eds.: M. Nicolini, U. Mazzi), SGE, Padova, **1999**, pp. 3–17.
- [2] a) E. Deutsch, K. Libson, J.-L. Vanderheyden, A. R. Ketrang, H. R. Maxon, *Nucl. Med. Biol.* **1986**, *13*, 465–477; b) E. Deutsch, K. Libson, J.-L. Vanderheyden in *Technetium and Rhenium in Chemistry and Nuclear Medicine*, Vol. 3 (Eds.: M. Nicolini, G. Bandoli, U. Mazzi), SGE, Padova, **1990**, pp. 13–22.
- [3] J. Dilworth, S. Parrot, *Chem. Soc. Rev.* **1998**, *27*, 43–55.
- [4] H. Spies, J.-H. Pietzsch, B. Johannsen in *Technetium, Rhenium and Other Metals in Chemistry and Nuclear Medicine*, Vol. 5 (Eds.: M. Nicolini, U. Mazzi), SGE, Padova, **1999**, pp. 101–108, and references therein.
- [5] a) I. Pirmettis, M. Papadopoulos, S. Mastrostamatis, C. P. Raptopoulou, A. Terzis, E. Chiotellis, *Inorg. Chem.* **1996**, *35*, 1685–1691; b) I. Pirmettis, M. Papadopoulos, E. Chiotellis, *J. Med. Chem.* **1997**, *40*, 2539–2546.
- [6] a) B. Johannsen, M. Sheunemann, H. Spies, P. Brust, J. Wober, R. Syhre, H.-J. Pietzsch, *Nucl. Med. Biol.* **1996**, *23*, 429–438; b) H.-J. Pietzsch, M. Sheunemann, M. Kretzschmar, S. Elz, H. Pertz, S. Seifert, P. Brust, H. Spies, R. Syhre, B. Johannsen, *Nucl. Med. Biol.* **1999**, *26*, 865–875; c) S. Meegala, K. Plossl, M.-P. Kung, A. D. Stevenson, L. M. Liable-Sands, A. L. Rheingold, H. F. Kung, *J. Am. Chem. Soc.* **1995**, *117*, 11037–11038; d) S. Meegala, K. Plossl, M.-P. Kung, S. Chumpradit, A. D. Stevenson, D. Frederick, H. F. Kung, *Bioconjugate Chem.* **1996**, *7*, 421–429.
- [7] a) A. Rey, I. Pirmettis, M. Pelecanou, M. Papadopoulos, C. P. Raptopoulou, L. Mallo, C. I. Stassinopoulou, A. Terzis, E. Chiotellis, A. Leon, *Inorg. Chem.* **2000**, *39*, 4211–4218; b) P. Bouziotis, I. Pirmettis, M. Papadopoulos, C. Tsoukalas, T. Maina, C. P. Raptopoulou, A. Terzis, E. Chiotellis, *Eur. J. Nucl. Med.* **1999**, *26*, 1194.
- [8] M. Papadopoulos, I. Pirmettis, M. Pelecanou, C. P. Raptopoulou, A. Terzis, C. I. Stassinopoulou, E. Chiotellis, *Inorg. Chem.* **1996**, *35*, 7377–7383.

- [9] H. R. Snyder, J. M. Steward, J. B. Ziegler, *J. Am. Chem. Soc.* **1947**, *69*, 2672–2674.
- [10] J. Chatt, G. A. Rowe, *J. Chem. Soc.* **1962**, 4019–4033.
- [11] B. Noll, T. Kniess, M. Friebe, H. Spies, B. Johannsen B. *Isot. Environ. Health Stud.* **1996**, *32*, 21–29.
- [12] T. N. Rao, D. Adhikesavalu, A. Camerman, A. R. Fritzberg, *Inorg. Chim. Acta* **1991**, *180*, 63–67.
- [13] a) T. N. Rao, D. Adhikesavalu, A. Camerman, A. R. Fritzberg, *J. Am. Chem. Soc.* **1990**, *112*, 5798–5804; b) B. Chen, M. Heeg, E. Deutsch, *Inorg. Chem.* **1992**, *31*, 4683–4690; c) F. Tisato, U. Mazzi, G. Bandoli, G. Cros, M. H. Darbieu, Y. Coulais, R. Giraud, *J. Chem. Soc. Dalton Trans.* **1991**, 1301–1307; d) J. O'Neil, S. Wilson, J. Katzenellenbogen, *Inorg. Chem.* **1994**, *33*, 319–323.
- [14] B. Johannsen, H. Spies in *Chemie und Radiopharmakologie von technetium komplexen*, Akademie der Wissenschaften der DDR, Rossendorf, **1981**, p. 213.
- [15] a) D. M. Spyriounis, M. Pelecanou, C. I. Stassinopoulou, C. P. Raptopoulou, A. Terzis, E. Chiotellis, *Inorg. Chem.* **1995**, *34*, 1077–1082; b) M. S. Papadopoulos, M. Pelecanou, I. C. Pirmettis, D. M. Spyriounis, C. P. Raptopoulou, A. Terzis, C. I. Stassinopoulou, E. Chiotellis, *Inorg. Chem.* **1996**, *35*, 4478–4483.
- [16] A. W. Addison, T. N. Rao, J. Reedijk, J. van Rijn, G. C. Verschoor, *J. Chem. Soc. Dalton Trans.* **1984**, 1349–1356.
- [17] a) A. Davison, A. Jones, C. Orvig, M. Sohn, *Inorg. Chem.* **1981**, *20*, 1629–1632; b) G. Bandoli, U. Mazzi, E. Roncari, E. Deutsch, *Coord. Chem. Rev.* **1982**, *44*, 191–227; c) M. Melnic, J. E. Van Lier, *Coord. Chem. Rev.* **1987**, *77*, 275–324; d) Y. Ohmoro, L. Francesconi, M-P. Kung, H. F. Kung, *J. Med. Chem.* **1992**, *35*, 157–162.
- [18] a) M. Pelecanou, I. C. Pirmettis, M. S. Papadopoulos, C. P. Raptopoulou, A. Terzis, E. Chiotellis, C. I. Stassinopoulou, *Inorg. Chim. Acta* **1999**, *287*, 142–151.
- [19] a) M. Pelecanou, K. Chryssou, C. I. Stassinopoulou, *J. Inorg. Biochem.* **2000**, *79*, 347–351; b) C. I. Stassinopoulou, M. Pelecanou, S. Mastrotamatis, E. Chiotellis, *Magn. Reson. Chem.* **1994**, *32*, 532–536.
- [20] D. L. Johnson, A. R. Fritzberg, B. L. Hawkins, S. Kasina, D. Eshima, *Inorg. Chem.* **1984**, *23*, 4204–4207.
- [21] G. M. Sheldrick, *SHELXS-86: Structure Solving Program*, University of Gottingen, Germany, **1986**.
- [22] G. M. Sheldrick, *SHELXL-93: Crystal Structure Refinement*, University of Gottingen, Germany, **1993**.

Received: November 13, 2000  
Revised: April 11, 2001 [F2864]